

Light-modulated graphene-based φ_{0} Josephson junction and $ -\varphi_{\bf 0}$ to $\varphi_{\bf 0}$ transition

Renxiang Cheng(程任翔), Miao Yu(于苗), Hong Wang(汪洪), Deliang Cao(曹德亮), Xingao Li(李兴鳌), Fenghua Qi(戚凤华), and Xingfei Zhou(周兴飞)

Citation: Chin. Phys. B, 2024, 33 (**2**): 027302. DOI: 10.1088/1674-1056/ad04c5
Journal homepage: http://cpb.iphy.ac.cn; http://iopscience.iop.org/cpb

What follows is a list of articles you may be interested in

Effects of strain on the flat band in twisted bilayer graphene

Zhen Zhang(张镇), Lu Wen(文露), Youkai Qiao(乔友凯), and Zhiqiang Li(李志强)
Chin. Phys. B, 2023, 32 (**10**): 107302. DOI: 10.1088/1674-1056/acb2c1

Epitaxial growth of trilayer graphene moiré superlattice

Yalong Yuan(袁亚龙), Yanbang Chu(褚衍邦), Cheng Hu(胡成), Jinpeng Tian(田金朋), Le Liu(刘乐), Fanfan Wu(吴帆帆), Yiru Ji(季怡汝), Jiaojiao Zhao(赵交交), Zhiheng Huang(黄智恒), Xiaozhou Zan(昝晓洲), Luojun Du(杜罗军), Kenji Watanabe, Takashi Taniguchi, Dongxia Shi(时东霞), Zhiwen Shi(史志文), Wei Yang(杨威), and Guangyu Zhang(张广宇)
Chin. Phys. B, 2023, 32 (**7**): 077304. DOI: 10.1088/1674-1056/accdc8

Gate-controlled localization to delocalization transition of flat band wavefunction in twisted monolayer-bilayer graphene

Siyu Li(李思宇), Zhengwen Wang(王政文), Yucheng Xue(薛禹承), Lu Cao(曹路), Kenji Watanabe, Takashi Taniguchi, Hongjun Gao(高鸿钧), and Jinhai Mao(毛金海)
Chin. Phys. B, 2023, 32 (**6**): 067304. DOI: 10.1088/1674-1056/acc805

Machine learning of the *Γ*-point gap and flat bands of twisted bilayer graphene at arbitrary angles

Xiaoyi Ma(马宵怡), Yufeng Luo(罗宇峰), Mengke Li(李梦可), Wenyan Jiao(焦文艳), Hongmei Yuan(袁红梅), Huijun Liu(刘惠军), and Ying Fang(方颖)
Chin. Phys. B, 2023, 32 (**5**): 057306. DOI: 10.1088/1674-1056/acb2c3

Spin- and valley-polarized Goos-Hänchen-like shift in ferromagnetic mass graphene junction with circularly polarized light

Mei-Rong Liu(刘美荣), Zheng-Fang Liu(刘正方), Ruo-Long Zhang(张若龙), Xian-Bo Xiao(肖贤波), and Qing-Ping Wu(伍清萍)
Chin. Phys. B, 2023, 32 (**3**): 037301. DOI: 10.1088/1674-1056/ac89e2

Light-modulated graphene-based φ_0 Josephson junction and $-\varphi_0$ to φ_0 transition

Renxiang Cheng(程任翔)[1,2], Miao Yu(于苗)[1], Hong Wang(汪洪)[1], Deliang Cao(曹德亮)[1], Xingao Li(李兴鳌)[1,†], Fenghua Qi(戚凤华)[3,‡], and Xingfei Zhou(周兴飞)[1,§]

[1] *New Energy Technology Engineering Laboratory of Jiangsu Province, School of Science, Nanjing University of Posts and Telecommunications, Nanjing* 210023, *China*

[2] *School of Electronic and Information Engineering, Jinling Institute of Technology, Nanjing* 211169, *China*

[3] *School of Electronic Engineering, Nanjing Xiaozhuang University, Nanjing* 211171, *China*

(Received 13 July 2023; revised manuscript received 8 September 2023; accepted manuscript online 19 October 2023)

We investigate the chiral edge states-induced Josephson current–phase relation in a graphene-based Josephson junction modulated by the off-resonant circularly polarized light and the staggered sublattice potential. By solving the Bogoliubov–de Gennes equation, a φ_0 Josephson junction is induced in the coaction of the off-resonant circularly polarized light and the staggered sublattice potential, which arises from the fact that the center of-mass wave vector of Cooper pair becomes finite and the opposite center of-mass wave vector to compensate is lacking in the nonsuperconducting region. Interestingly, when the direction of polarization of light is changed, $-\varphi_0$ to φ_0 transition generates, which generalizes the concept of traditional 0–π transition. Our findings provide a purely optical way to manipulate a phase-controllable Josephson device and guidelines for future experiments to confirm the presence of graphene-based φ_0 Josephson junction.

Keywords: graphene, circularly polarized light, staggered sublattice potential, φ_0 Josephson junction

PACS: 73.22.Pr, 73.20.At, 78.67.–n, 85.25.–j **DOI:** 10.1088/1674-1056/ad04c5

1. Introduction

Graphene, a flat monolayer of carbon atoms arranged in a two-dimensional (2D) honeycomb lattice, was studied theoretically in 1947.[1] It was viewed as a thriving theoretical toy model until the realization of graphene in experiment in 2004.[2] By using the tight-binding model, there are two inequivalent corners K and K' in the first Brillouin zone, around which is a conical band structure described by the massless Dirac equation.[3] Owing to its linear electronic spectrum, graphene has become a new type of "relativistic" material, where some unobservable relativistic phenomena in high energy physics, such as Klein tunneling and anomalous Klein tunneling,[4–8] can be easily mimicked and tested in condensed matter physics. Graphene not only provides a highly practical and prospective platform for studying fundamental physics, such as half-integer quantum Hall effect,[9] specular Andreev reflection,[10] topological phase transition,[11–14] and superconductivity,[15–18] but also has extraordinary applications in future, such as next-generation electronics and photonics,[19,20] device physics,[21] and heterostructure.[22] With the rise of graphene, the research about two dimensional materials, such as silicene,[23] 2D transition metal dichalcogenides,[24–26] and phosphorene,[27,28] flourishes and continues to provide a fertile ground for applications such as energy storage and novel topological electronic devices.[29–31]

Josephson effect, the flow of supercurrent between two pieces of superconducting material separated by a thin layer of insulating material, was first predicted by English physicist Josephson and then was verified in experiment by Anderson and Rowell.[32,33] In this case, the minimal Josephson free energy appears at zero phase difference by calculating the phase-difference-dependent Josephson free energy, which is called 0 Josephson junction. When the insulating material is replaced by a ferromagnetic metal, i.e., superconductor-ferromagnet-superconductor junction, the minimal Josephson free energy may appear at π phase difference and the direction of the critical supercurrent may be reversed, which is called 0–π transition and is suggested as a promising device to realize qubits.[34–36] When the minimal Josephson free energy appears at φ_0 phase difference ($\varphi_0 \neq 0, \pi$), the finite supercurrent exists at zero phase difference. This Josepshon junction called φ_0 Josephson junction with an unconventional supercurrent-phase relation $J = J_c \sin(\phi - \varphi_0)$, which was discussed in the nanowire-based Josephson junction applied by the Rashba spin–orbit coupling and the Zeeman field,[37,38] the magnetic field-modulated quantum spin-Hall insulator,[39] the one-dimensional topological interface states constructed in a 2D honeycomb-lattice system,[40] the magnetized topological insulator interfaces,[41] the electrically modulated silicene nanoribbon,[42] a Bi_2Se_3-based Josephson junction in the presence of an in-plane magnetic field,[43] and

†Corresponding author. E-mail: lixa@njupt.edu.cn
‡Corresponding author. E-mail: qifenghua@njxzc.edu.cn
§Corresponding author. E-mail: zxf@njupt.edu.cn

© 2024 Chinese Physical Society and IOP Publishing Ltd

the quantum anomalous Hall insulator.[44] These Josephson junctions play an important role in the design of superconducting circuits,[45–48] which stimulates researchers to study the Josephson effect constantly.

The graphene-based Josephson junction was studied widely.[49–54] The bipolar supercurrent in graphene was observed.[50] A π Josephson junction was predicted.[51] The PbIn–graphene–PbIn Josephson junction would facilitate the development of superconducting quantum information devices.[52] Supercurrent rectification effect in graphene-based Josephson junctions was discussed.[53] Electric controlled φ_0 Josephson junction was investigated in twisted bilayer graphene in theory.[54] However, the realizations of topological edge states-induced φ_0 Josephson junction in graphene were rare. Although the edge states-induced φ_0 Josephson junction were discussed in silicene and other 2D materials,[40,42,44] the realization of superconductivity in graphene is easier than the one in this materials experimentally. So, in this work, we discuss how to realize topological edge states-induced φ_0 Josephson junction in graphene. The schematic diagrams for graphene-based Josephson junction is shown in Fig. 1. The chiral edge states is induced by the off-resonant circularly polarized light, which was studied in both theory and experiment.[55,56] The staggered sublattice potential induced by SiC substrate will modulate the chiral edge states in the middle region,[13] which is the key point for the realization of φ_0 Josephson junction.

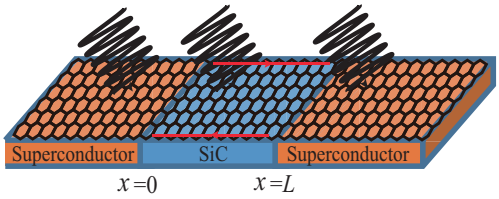


Fig. 1. Schematic diagram for graphene-based Josephson junction. The zigzag graphene nanoribbon is divided into three regions consist of two superconducting regions and a normal region. The superconductivity in left and right regions are realized by applying an s-wave superconductor. In the normal region, the graphene nanoribbon is deposited on an SiC substrate. The off-resonant circularly polarized light irradiates three regions. The chiral edges with spin degeneracy are shown in the middle region.

The paper is organized as follows. We firstly give the model and basic formalism. Then, the numerical results and theoretical analysis are presented and discussed. Finally, the main results of this work are summarized.

2. Models and methods

We consider a zigzag graphene nanoribbon which is deposited on an SiC substrate and irradiated by an off-resonant circularly polarized light. The Hamiltonian of the zigzag graphene nanoribbon is

$$H = -t\sum_{\langle i,j\rangle} c_i^{\dagger}c_j + \Delta\sum_i \mu_i c_i^{\dagger}c_i + \mathrm{i}\frac{\eta\Delta_\omega}{3\sqrt{3}}\sum_{\langle\langle i,j\rangle\rangle} v_{ij}c_i^{\dagger}c_j. \quad (1)$$

The first term of Eq. (1) is the nearest-neighbor hopping of electron with the creation (annihilation) operator $c_{i(j)}^{\dagger}$ ($c_{i(j)}$) at i (j) site and the hopping integral $t = 2.82$ eV. The symbols $\langle i,j\rangle$ and $\langle\langle i,j\rangle\rangle$ represent nearest neighbors and next-nearest neighbors, respectively. The second term of Eq. (1) denotes the staggered sublattice potential term with the site energy Δ and the sublattice index $\mu_i = 1$ (-1) for A (B) sublattice. The third term of Eq. (1) is the Haldane term which is induced by the off-resonant irradiation with the illumination parameter Δ_ω. $\eta = 1$ (-1) represents the right (left) circularly polarized light. When the next-nearest-neighbor hopping is anticlockwise (clockwise) in the plane, the symbol v_{ij} is equal to 1 (-1).

According to the tight-binding model, the energy bands of zigzag graphene nanoribbon with different parameters Δ and Δ_ω are shown in Fig. 2. The quantum anomalous Hall effect is induced by irradiating off-resonant left (right) circularly polarized light, shown in Figs. 2(a) and 2(b).

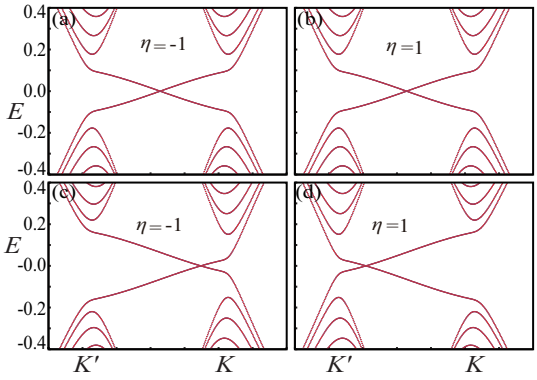


Fig. 2. Dispersion relations of a zigzag graphene nanoribbon by irradiating off-resonant left (right) circularly polarized light for panels (a)–(c) ((b)–(d)). (a)–(b) There is no SiC substrate. (c)–(d) There is an SiC substrate. The unit for energy is 1 eV and the width of nanoribbon $W = 60$ atoms.

It is obvious that the light-induced edge states are independent of the polarization of light. But, when the staggered sublattice potential is considered, shown in Figs. 2(c) and 2(d), the light-induced edge states are dependent on the polarization of light. The intersection of edge states moves to K (K') valley when the left (right) circularly polarized light is irradiated on the zigzag graphene nanoribbon. In order to investigate the properties of edge states modulated by the cooperation of the off-resonant light and the staggered sublattice potential, the uniform Hamiltonian for top and bottom edge states is approximately given as[57,58]

$$\mathcal{H}_s = s(\hbar v k_x + \eta\Delta), \quad (2)$$

where $s = +$ ($-$) denotes the top (bottom) edge state, Δ is the site energy of sublattice from the contribution of SiC substrate, and the velocity approximately equals the light-induced gap divided by the distance of two valleys, i.e., $v = (\sqrt{3}\Delta_\omega/\pi t)v_F$ with light-induced gap Δ_ω, the hopping integral $t = 2.82$ eV, and the Fermi velocity $v_F = 1\times10^6$ m/s.

In our system, shown in Fig. 1, the electron and hole excitations are described by the Bogoliubov–de Gennes (BdG) equation

$$\begin{pmatrix} \mathcal{H}_s(k_x) - E_{\rm F} & \Delta' \\ \Delta'^{*} & E_{\rm F} - \mathcal{H}_{\bar{s}}(-k_x) \end{pmatrix} \begin{pmatrix} u_{\rm e} \\ v_{\rm h} \end{pmatrix} = \varepsilon \begin{pmatrix} u_{\rm e} \\ v_{\rm h} \end{pmatrix}, \quad (3)$$

where the basis vector of BdG Hamiltonian is $(c_{k\sigma}, c^{\dagger}_{-k\bar{\sigma}})^{\dagger}$ with $c_{k\sigma}$ ($c^{\dagger}_{-k\bar{\sigma}}$) annihilating (creating) an electron with spin index σ ($\bar{\sigma}$) and momentum k ($-k$). Here we ignore the spin index in BdG equation due to the spin degeneracy. $\mathcal{H}_s = s[\hbar v k_x + \eta\Delta(\Theta(x-L/2)+\Theta(x+L/2))]$ with the Heaviside step function $\Theta(x)$. $E_{\rm F}$ is the Fermi energy of system. ε is the excited energy (relative to the Fermi energy) of electron and hole. $u_{\rm e}$ and $v_{\rm h}$ represent the electron and hole wavefunctions in the normal region, respectively. In the superconducting region, $u_{\rm e}$ and $v_{\rm h}$ denote the electron-like and hole-like wavefunctions, respectively. $\Delta' = \Delta_0 \mathrm{e}^{\mathrm{i}\phi_{\rm L\,(R)}}$ in the left (right) superconducting region with the zero temperature energy-gap function of s-wave superconductor Δ_0 and the phase $\phi_{\rm L\,(R)}$. For the convenience of discussion, we consider the set with $\mathcal{H}_+$ due to the symmetry of edges. By solving Eq. (3), the excited spectrum of electron and hole in the middle region are derived as

$$\varepsilon_{\rm e} = \hbar v k_x^{\rm e} + \eta\Delta - E_{\rm F}, \quad \varepsilon_{\rm h} = -\hbar v k_x^{\rm h} + \eta\Delta + E_{\rm F}. \quad (4)$$

The uniform spectrum in both superconducting regions is

$$\varepsilon = \sqrt{(\hbar v k_x^s - E_{\rm F})^2 + \Delta_0^2}. \quad (5)$$

The wavefunctions of electron and hole in the middle regions are

$$\psi_{\rm e} = \mathrm{e}^{\mathrm{i}k_x^{\rm e}}(1,0)^{\rm T}, \quad \psi_{\rm h} = \mathrm{e}^{\mathrm{i}k_x^{\rm h}}(0,1)^{\rm T}. \quad (6)$$

The wavevectors of electron and hole are given by Eq. (4)

$$k_x^{\rm e} = \frac{\varepsilon - \eta\Delta + E_{\rm F}}{\hbar v}, \quad k_x^{\rm h} = -\frac{\varepsilon - \eta\Delta - E_{\rm F}}{\hbar v}. \quad (7)$$

The eigenstates of qausiparticle in left and right superconducting regions are

$$\psi^{\pm}_{\rm SL\,(R)} = \mathrm{e}^{\mathrm{i}k_s^{\pm}x}(\mathrm{e}^{\pm\mathrm{i}\beta}, \mathrm{e}^{-\mathrm{i}\phi_{\rm L\,(R)}})^{\rm T}, \quad (8)$$

where $+$ $(-)$ represents quasi-electron (quasi-hole) wavefunction. The wavevector of quasiparticle $k_s^{\pm}$ is derived as $(E_{\rm F} \pm \sqrt{\varepsilon^2 - \Delta_0^2})/\hbar v$ through Eq. (5). When $\varepsilon < \Delta_0$, $\beta = \arccos(\varepsilon/\Delta_0)$. When $\varepsilon > \Delta_0$, $\beta = -\mathrm{i}\,\mathrm{arcosh}(\varepsilon/\Delta_0)$.

In the short-junction regime, due to the continuity of wavefunction at interface, the wavefunctions in both middle and superconducting regions at interfaces are continuous, i.e., $r\psi^{-}_{\rm SL}|_{x=0} = \Psi|_{x=0}$ and $t\psi^{+}_{\rm SR}|_{x=L} = \Psi|_{x=L}$ in which $\Psi = a\psi_{\rm e} + b\psi_{\rm h}$ and r, a, b, and t are the probability amplitudes of the corresponding wavefunctions. Obviously, when r, a, b, and t are treated as four variables, there is a system of linear equations made up of four equations. In order to ensure the nonzero solution, the value of determinant of coefficients is equal to zero. Thus, we obtain

$$\sin\frac{1}{2}[(k_x^{\rm e} - k_x^{\rm h})L - 2\beta + \phi] = 0, \quad (9)$$

where $\phi = \phi_{\rm L} - \phi_{\rm R}$ is the phase difference between left and right superconductors. From the above equation, it is easy to obtain $(1/2)[(k_{\rm e} - k_{\rm h})L - 2\beta + \phi] = n\pi$ with integer n. By some calculations, we can get

$$\varepsilon = \pm\Delta_0 \cos(1/2)[(k_{\rm e} - k_{\rm h})L + \phi]. \quad (10)$$

These levels are called Andreev bound state (ABS) levels which make the Cooper pair cross the normal region.

3. Results and discussion

3.1. Andreev bound state levels

In the short-junction regime, The ABS levels are calculated by Eq. (10)

$$\varepsilon = \pm\Delta_0 \cos\left(\frac{\phi}{2} - \frac{\eta\Delta L}{\hbar v}\right). \quad (11)$$

It is obvious that the effective phase shift happens in the coaction of left (right) circularly polarized light and SiC substrate. The phase difference-ABS levels are shown in Fig. 3. The ABS levels are symmetric about phase difference $\phi = \pi$ without SiC substrate, shown in Figs. 3(a) and 3(b). In other words, there is no phase shift in the presence of only polarized light. In addition, it is difficult to distinguish the effect of left circularly polarized light and right circularly polarized light from Figs. 3(a) and 3(b). In the coaction of left (right) circularly polarized light and SiC substrate, shown in Figs. 3(c) and 3(d), the effective phase shift happens and the directions of phase shift for two types of circularly polarized light are opposite, which aries from the fact that the direction of valley polarization is dependent on the polarized direction of light, shown in Figs. 2(c) and 2(d). By using the values of parameters in Fig. 3, the effective phase shift can be estimated by Eq. (11), i.e., $2[\eta(\Delta L/\hbar v)\mathrm{mod}\,2\pi] + \pi$. It is easy to obtain that the effective phase shift is approximately equal to 2.6505 (3.6325) for left (right) circularly polarized light, which are well consistent with the numerical results in Figs. 3(c) and 3(d). According to the periodicity of Eq. (11), the effective phase shift is approximately equal to $2[\eta(\Delta L/\hbar v)\mathrm{mod}\,2\pi) \approx \eta 0.488$ for left (right) circularly polarized light, which indicates that the left circularly polarized light and the right circularly polarized light make the effective phase shift opposite completely. The effective phase shift will bring φ_0 junction.

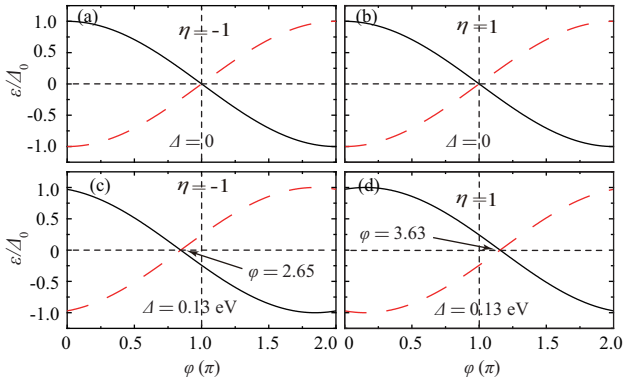


Fig. 3. (a)–(d) Andreev bound state levels *versus* the phase difference with illumination parameter $\Delta_\omega = 0.2$ eV. The black (red-dotted) line denotes Eq. (11) with positive (negative) sign. The junction length L is 10 nm.

3.2. The φ_0 junction and $-\varphi_0$ to φ_0 transition

According to Eq. (11), the relation between the Josephson current J and the positive ABS levels at zero temperature is given as[59]

$$J = -\frac{2e}{\hbar}\frac{\mathrm{d}\varepsilon}{\mathrm{d}\phi}. \tag{12}$$

Figure 4 shows the Josephson current as a function of the phase difference. The shape of black line reveals the Josephson junction is a traditional 0 junction in the presence of off-resonant circularly polarized light without substrate, which is consistent with the characteristic of ABS levels in Figs. 3(a) and 3(b). In the coaction of off-resonant circularly polarized light and SiC substrate, from Eqs. (11) and (12), when phase difference $\phi = 0$,

$$J = +(-)\frac{e\Delta_0}{\hbar}\sin(-\eta\frac{\Delta L}{\hbar v})$$

as $\cos(-\eta(\Delta L/\hbar v)) > 0$ (< 0). By using the values of parameters in Fig. 3, when the left (right) circularly polarized light is irradiated in Josephson junction, the Josephson current is approximately equal to 0.241 (-0.241) as phase difference $\phi = 0$, which is consistent with the numerical results in Fig. 3 with red-dotted blue-dotted lines. This is the characteristic of φ_0 junction. By some simple calculations, it is easy to obtain $\varphi_0 = 2\eta[(\Delta L/\hbar v) \bmod 2\pi] \approx \eta 0.488$, which is consistent with the phase shift of ABS levels in Figs. 3(c) and 3(d).

Figure 5 shows the Josephson current as a function of the illumination parameter Δ_ω with the staggered sublattice potential $\Delta = 0.13$ eV and phase difference $\phi = 0$. The Josephson current displays a nondamped oscillation with variation of Δ_ω, which is consistent with Eq. (12) as $\phi = 0$. Interestingly, the behaviors of nondamped oscillation for left and right circularly polarized lights are opposite completely, which means that $-\varphi_0$ junction can be changed to φ_0 junction by modulating the direction of polarization of light. This is similar to the traditional 0–π transition. Thus, the transition phenomenon in Fig. 5 is called as $-\varphi_0$ to φ_0 transition, which is the generalization of 0–π transition. It is easy to make $-\varphi_0$ to φ_0 transition become 0–π transition by adjusting the illumination parameter Δ_ω and the direction of polarization of light.

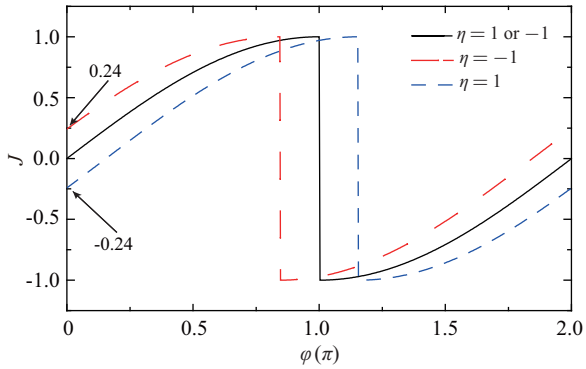


Fig. 4. Phase difference-dependent Josephson current with illumination parameter $\Delta_\omega = 0.2$ eV. The black line denotes the case of left (right) circularly polarized light without substrate. The red–dotted (blue–dotted) line denotes left (right) circularly polarized light with SiC substrate-induced gap $\Delta = 0.13$ eV. The unit for Josephson current is $e\Delta_0/\hbar$. The junction length L is 10 nm.

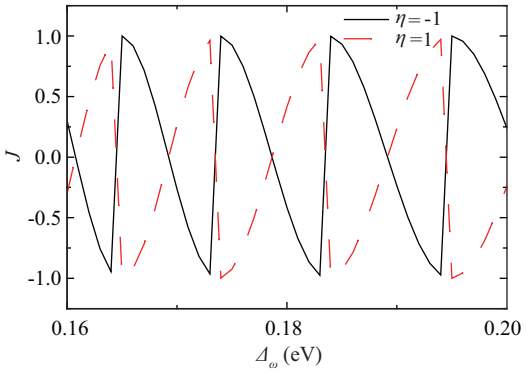


Fig. 5. Illumination parameter-dependent Josephson current with $\Delta = 0.13$ eV and phase difference $\phi = 0$. The black (red–dotted) line represents the case of left (right) circularly polarized light. The unit for Josephson current is $e\Delta_0/\hbar$. The junction length L is 10 nm.

In order to clarify $-\varphi_0$ to φ_0 transition clearly, we calculate the phase-dependent free energy of Josephson junction,[60] which is defined as

$$F = \frac{\hbar}{2e}\int_0^\phi J\,\mathrm{d}\phi.$$

The position of minimal free energy decides the type of Josephson junction. The minimal free energy is at $\phi = 0$ with $\Delta_\omega = 0.2$ eV and $\Delta = 0$, which is called 0 junction and shown in Fig. 6 with black line. When the staggered sublattice potential is considered, shown in Fig. 6 with red–dotted (blue–dotted) line, the minimal free energy is at $\phi = 0.49$ (-0.49) in the presence of right (left) circularly polarized light, which is well consistent with the analytical solution $(\varphi_0 = 2\eta[(\Delta L/\hbar v) \bmod 2\pi] \approx \eta 0.488)$ from Eq. (11). It is obvious to find that the type of Josephson junction transitions from 0.49 junction to -0.49 junction by changing the direction of polarization of light, shown in Fig. 6, which is similar to the case that the type of Josephson junction transitions from 0 junction to π junction (0–π transition). So, the transition in

our paper is called $-\varphi_0$ to φ_0 transition, which generalizes the concept of 0–π transition. The difference between these two types of transition is that the transition of Josephson current at zero phase difference is the signature of $-\varphi_0$ to φ_0 transition (shown in Fig. 5) while the critical current transition is the signature of 0–π transition.

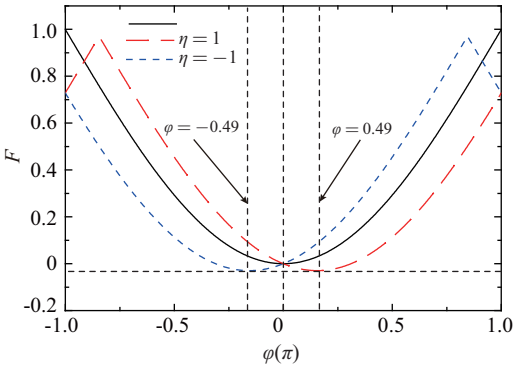


Fig. 6. Phase-dependent free energy of Josephson junction with $\Delta_\omega = 0.2$ eV. The black line represents the case of left or right circularly polarized light without staggered sublattice potential. The red–dotted (blue–dotted) denotes the case of left (right) circularly polarized light with staggered sublattice ($\Delta = 0.13$ eV). The unit for free energy is Δ_0. The junction length L is 10 nm.

4. Conclusion

In conclusion, a light-modulated topological edge states-induced φ_0 junction is found in a graphene-based Josephson junction. In the nonsuperconducting region, the center of-mass wave vector of Cooper pair becomes finite and the opposite center of-mass wave vector to compensate is lacking in the coaction of the circularly polarized light and the staggered sublattice potential, which is the physical origin of φ_0 junction. In addition, by changing the direction of polarization of light, $-\varphi_0$ to φ_0 transition is found, which generalizes the concept of traditional 0–π transition. These results provide experimental proposals to realize graphene-based φ_0 Josephson junction and promise potential applications in phase-controllable Josephson devices.

Acknowledgements

Project supported by the National Natural Science Foundation of China (Grant Nos. 12104232, 11805103, and 11804167), the Natural Science Foundation of Jiangsu Province, China (Grant Nos. BK20190137 and BK20180739), the Fundamental Research Funds for the Central Universities (Grant Nos. 020414380195 and B230201042), the Jit-b Project (Grant No. 201831), and the Natural Science Fund of Nanjing University of Posts and Telecommunications (Grant No. NY222163).

References

[1] Wallace P R 1947 *Phys. Rev.* **71** 622
[2] Novoselov K S, Geim A K, Morozov S V, Jiang D, Zhang Y, Dubonos S V, Grigorieva I V and Firsov A A 2004 *Science* **306** 666
[3] Castro Neto A H, Guinea F, Peres N M R, Novoselov K S and Geim A K 2009 *Rev. Mod. Phys.* **81** 109
[4] Katsnelson M I, Novoselov K S and Geim A K 2006 *Nat. Phys.* **2** 620
[5] Zeb M A, Sabeeh K and Tahir M 2008 *Phys. Rev. B* **78** 165420
[6] Stander N, Huard B and Goldhaber-Gordon D 2009 *Phys. Rev. Lett.* **102** 026807
[7] Rozhkov A, Giavaras G, Bliokh Y P, Freilikher V and Nori F 2011 *Phys. Rep.* **503** 77
[8] Zhou X, Wu Z, Bai Y, Wang Q, Zhu Z, Yan W and Xu Y 2022 *Chin. Phys. B* **31** 047301
[9] Zhang Y, Tan Y W, Stormer H L and Kim P 2005 *Nature* **438** 201
[10] Beenakker C W J 2006 *Phys. Rev. Lett.* **97** 067007
[11] Kane C L and Mele E J 2005 *Phys. Rev. Lett.* **95** 146802
[12] Qiao Z, Tse W K, Jiang H, Yao Y and Niu Q 2011 *Phys. Rev. Lett.* **107** 256801
[13] Zhai X and Jin G 2014 *Phys. Rev. B* **89** 235416
[14] Wang W, Lü X and Xie H 2021 *Chin. Phys. B* **30** 066701
[15] Bistritzer R and MacDonald A H 2011 *Proc. Natl. Acad. Sci. USA* **108** 12233
[16] Cao Y, Fatemi V, Fang S, Watanabe K, Taniguchi T, Kaxiras E and Jarillo-Herrero P 2018 *Nature* **556** 43
[17] Tarnopolsky G, Kruchkov A J and Vishwanath A 2019 *Phys. Rev. Lett.* **122** 106405
[18] Yankowitz M, Chen S, Polshyn H, Watanabe K, Taniguchi T, Graf D, Young A F and Dean C R 2019 *Science* **363** 11059
[19] García de Abajo F J 2013 *Science* **339** 917
[20] Koppens F, Mueller T, Avouris P, Ferrari A, Vitiello M and Polini M 2014 *Nat. Nanotechnol.* **9** 780
[21] Wolf E L 2014 *Graphene: A New Paradigm in Condensed Matter and Device Physics* (Oxford: Oxford University Press)
[22] Young A F and Kim P 2011 *Annual Review of Condensed Matter Physics* **2** 101
[23] Liu C C, Jiang H and Yao Y 2011 *Phys. Rev. B* **84** 195430
[24] Wang Q H, Kalantar-Zadeh K, Kis A, Coleman J N and Strano M S 2012 *Nat. Nanotechnol.* **7** 699
[25] Xu X, Yao W, Xiao D and Heinz T F 2014 *Nat. Phys.* **10** 343
[26] Manzeli S, Ovchinnikov D, Pasquier D, Yazyev O V and Kis A 2017 *Nat. Rev. Mater.* **2** 17033
[27] Li L, Yu Y, Ye G J, Ge Q, Ou X, Wu H, Feng D, Chen X H and Zhang Y 2014 *Nat. Nanotechnol.* **9** 372
[28] Carvalho A, Wang M, Zhu X, Rodin A S, Su H and Castro Neto A H 2016 *Nat. Rev. Mater.* **1** 16061
[29] Late D J, Huang Y K, Liu B, Acharya J, Shirodkar S N, Luo J, Yan A, Charles D, Waghmare U V, Dravid V P and Rao C N R 2013 *ACS Nano* **7** 4879
[30] Chhowalla M, Shin H S, Eda G, Li L J, Loh K P and Zhang H 2013 *Nat. Chem.* **5** 263
[31] Qian X, Liu J, Fu L and Li J 2014 *Science* **346** 1344
[32] Josephson B D 1962 *Phys. Lett.* **1** 251
[33] Anderson P W and Rowell J M 1963 *Phys. Rev. Lett.* **10** 230
[34] Ryazanov V V, Oboznov V A, Rusanov A Yu, Veretennikov A V, Golubov A A and Aarts J 2001 *Phys. Rev. Lett.* **86** 2427
[35] Buzdin A I 2005 *Rev. Mod. Phys.* **77** 935
[36] Yamashita T, Tanikawa K, Takahashi S and Maekawa S 2005 *Phys. Rev. Lett.* **95** 097001
[37] Yokoyama T, Eto M and Nazarov Y V 2014 *Phys. Rev. B* **89** 195407
[38] Nesterov K N, Houzet M and Meyer J S 2016 *Phys. Rev. B* **93** 174502
[39] Dolcini F, Houzet M and Meyer J S 2015 *Phys. Rev. B* **92** 035428
[40] Wang J, Hao L and Liu J F 2016 *Phys. Rev. B* **93** 155405
[41] Alidoust M and Hamzehpour H 2017 *Phys. Rev. B* **96** 165422
[42] Zhou X and Jin G 2107 *Phys. Rev. B* **95** 195419
[43] Assouline A, Feuillet-Palma C, Bergeal N, Zhang T, Mottaghizadeh A, Zimmers A, Lhuillier E, Eddrie M, Atkinson P, Aprili M and Aubin H 2019 *Nat. Commun.* **10** 126
[44] Xu Y, Fu P H, Chen L, Liu J F, Wang J and Xu H 2022 *Phys. Rev. B* **105** 075409
[45] Padurariu C and Nazarov Y V 2010 *Phys. Rev. B* **81** 144519
[46] Reynoso A A, Usaj G, Balseiro C A, Feinberg D and Avignon M 2012 *Phys. Rev. B* **86** 214519
[47] Gingrich E C, Niedzielski B M, Glick J A, Wang Y, Miller D L, Loloee R, Pratt Jr W P and Birge N O 2016 *Nat. Phys.* **12** 564
[48] Strambini E, Iorio A, Durante O, Citro R, Sanz-Fernández C, Guarcello C, Tokatly I V, Braggio A, Rocci M, Ligato N, Zannier V, Sorba L, Bergeret F S and Giazotto F 2020 *Nat. Nanotechnol.* **15** 656
[49] Titov M and Beenakker C W J 2006 *Phys. Rev. B* **74** 041401

[50] Heersche H B, Jarillo-Herrero P, Oostinga J B, Vandersypen L M K and Morpurgo A F 2007 *Nature* **446** 56
[51] Linder J, Yokoyama T, Huertas-Hernando D and Sudbø A 2008 *Phys. Rev. Lett.* **100** 187004
[52] Jeong D, Choi J H, Lee G H, Jo S, Doh Y J and Lee H J 2011 *Phys. Rev. B* **83** 094503
[53] Wei Y J, Liu H L, Wang J and Liu J F 2022 *Phys. Rev. B* **106** 165419
[54] Xie Y M, Efetov D K and Law K T 2022 *Phys. Rev. Res.* **5** 023029
[55] Kitagawa T, Oka T, Brataas A, Fu L and Demler E 2011 *Phys. Rev. B* **84** 235108
[56] McIver J W, Schulte B, Stein F U, Matsuyama T, Jotzu G, Meier G and Cavalleri A 2020 *Nat. Phys.* **16** 38
[57] Drummond N D, Zólyomi V and Fal'ko V I 2012 *Phys. Rev. B* **85** 075423
[58] Xu Y and Jin G 2017 *Phys. Rev. B* **95** 155425
[59] Beenakker C W J 1991 *Phys. Rev. Lett.* **67** 3836
[60] nnunziata G, Enoksen H, Linder J, Cuoco M, Noce C and Sudbø A 2011 *Phys. Rev. B* **83** 144520